Available on: https://jnsrr.ep-journals.org/ E-ISSN: 3051-3766 P-ISSN: 3051-3758

Journal of Natural Science Research and Review

Volume: 02 Issue: 11 November-2026

Disordered Hyperuniform States from A Phase-Field-Crystal Model with A Stochastic Characteristic Wavenumber

Nkosikhona Dlamini
Department of Physics, University of Eswatini, Kwaluseni, Eswatini

Sebenzile Tsabedze
Department of Physics, University of Eswatini, Kwaluseni, Eswatini

Simiso K. Mkhonta
Department of Physics, University of Eswatini, Kwaluseni, Eswatini

Published Date: November 11, 2026 **Article DOI: 10.65150/EP-jnsrr/V2E11/2026-02**

ABSTRACT: Disordered hyperuniform systems are disordered configurations that suppress density fluctuations at large length scales while lacking the conventional long-range translational order characteristic of crystals. Developing computational approaches capable of generating and dynamically studying such structures is important for understanding their formation and for designing functional disordered materials. Here, we introduce and investigate a modified phase-field-crystal (PFC) model in which the characteristic wavenumber controlling the preferred lattice spacing is subjected to a spatially and temporally fluctuating perturbation. Starting from random initial conditions, the system evolves from a liquid-like state toward patterned states whose local structure remains approximately triangular while conventional long-range translational order is disrupted. The resulting structures are characterized using local number variance and pair-correlation functions. For perturbation amplitudes $0 \leq \delta \leq 0.20$, the number variance exhibits approximately linear scaling consistent with class-III hyperuniform behavior in two dimensions. At the same time, the pair-correlation function retains several well-defined short-range peaks while approaching unity at large separation, demonstrating the coexistence of local structural order and the absence of conventional long-range spatial correlations. The free-energy evolution follows an approximate power-law decay $E(t) \sim t^{\cdot}$, corresponding to a characteristic domain length scale $L \sim t^{\cdot}$. A numerical state diagram in the $r - \delta$ parameter space further demonstrates the persistence of the triangular state over a range of perturbation amplitudes, with larger perturbations promoting coexistence with other patterns. These results demonstrate that a stochastic characteristic wavenumber provides a simple computational mechanism for generating disordered hyperuniform states within a PFC framework and for studying their formation on diffusive time scales.

KEYWORDS: disordered hyperuniformity, phase-field crystal, stochastic wavenumber, pattern formation, free-energy dynamics, short-range order, computational materials.

1. INTRODUCTION

Disordered materials can display structural correlations that are not apparent from their visual disorder. A particularly important class is formed by disordered hyperuniform systems, which combine the absence of conventional long-range translational order with an anomalous suppression of density fluctuations at large length scales [1–5]. In an ordinary disordered system such as a liquid, the number of particles contained within an observation window fluctuates according to the volume of the window. In a two-dimensional Poisson-like system, for example, the number variance scales as the area of the observation window. Hyperuniform systems instead exhibit number fluctuations that grow more slowly than the volume of the observation window
[6,7].

This combination of disorder and suppressed long-wavelength fluctuations distinguishes hyperuniform structures from both conventional rystals and ordinary disordered systems. Crystals possess long-range translational order, whereas liquids and structural glasses generally exhibit strong density fluctuations at large length scales. Disordered hyperuniform configurations occupy an intermediate structural regime: they can appear statistically disordered while retaining hidden large-scale organization [1,6,8].

Hyperuniformity has been identified in a broad range of physical systems, including jammed particle assemblies, disordered ground states, biological structures, photonic materials, and nonequilibrium systems [9–18]. The structural characteristics of these systems can lead to unusual optical, transport, mechanical, and thermodynamic properties. In particular, hyperuniform disordered arrangements have attracted considerable interest for photonic applications because they can combine disorder with controlled suppression of long-wavelength density fluctuations [19–21].

License: This is an open access article under the CC BY 4.0 license: https://creativecommons.org/licenses/by/4.0/

An important problem is therefore the development of computational methods capable of generating and controlling disordered hyperuniform structures. Inverse-design approaches, particle-based models, and stochastic construction methods have all been used to address this problem [1,22,23]. However, many computational approaches focus on static configurations rather than on the dynamics through which the structures form. The phase-field-crystal (PFC) model provides a potentially useful framework for this purpose. PFC models describe a coarsegrained density field while retaining microscopic length scales and allowing simulations over diffusive time scales [24–27]. They have been widely used to study crystallization, grain growth, epitaxial growth, defect dynamics, and other processes involving crystalline structures. The principal advantage of the PFC approach in the present context is that it provides a computationally efficient description of pattern formation at length scales associated with microscopic structure while permitting access to substantially longer diffusive time scales than conventional molecular-dynamics simulations. The standard two-dimensional PFC model supports several characteristic states, including a homogeneous liquid-like state, a triangular or hexagonal crystalline state, and a stripe state [26–29]. The periodic crystalline state arises because the free-energy functional contains a preferred characteristic wavenumber q , which establishes a characteristic structural length scale.

In this work, we modify this mechanism by allowing the characteristic wavenumber itself to fluctuate. Rather than imposing a single fixed structural wavelength, we introduce a stochastic characteristic wavenumber. The resulting local fluctuations in the preferred wavelength provide a simple route for disrupting conventional periodic order while retaining the underlying tendency toward local pattern formation.

The objective is to determine whether this stochastic-wavenumber PFC model can generate disordered hyperuniform structures and, if so, to characterize their structural and dynamical properties. We further examine the robustness of the resulting states as the perturbation amplitude is varied. The present study extends earlier work on uniformly randomized lattices, which demonstrated resilience of short-range order under static random positional perturbations [30]. In contrast, the present approach incorporates randomness directly into a dynamical PFC framework through the characteristic wavenumber, thereby providing a mechanism for generating and evolving disordered structures during free-energy relaxation.

2. MODEL AND NUMERICAL METHODOLOGY

2.1 Phase-field-crystal free energy

The PFC model describes the system using a continuous density-like field $\psi(r, t)$. The free-energy functional considered here is

$$F[\psi] = \int_{\Omega} d^d r \left[\frac{\psi}{2}\{r + \lambda(q_0^2 + \nabla^2)^2\}\psi - \frac{\psi^3}{3} + \frac{\psi^4}{4}\right], \quad (2.1)$$

where r is a reduced temperature-like parameter, λ is a phenomenological parameter, q is the characteristic wavenumber, and Ω denotes the computational domain.

The characteristic wavenumber determines the preferred structural wavelength.

For a fixed q , the corresponding characteristic lattice spacing is

$$a_0 = \frac{2\pi}{q_0}. \quad (2.2)$$

For conventional PFC dynamics, the order parameter can evolve according to either conserved or unconserved dynamics. The conserved form is associated with particle-number conservation, whereas the unconserved form corresponds to a Swift–Hohenbergtype relaxational dynamics.

In the present work, the unconserved dynamics are used:

$$\frac{\partial \psi}{\partial t} = -\mu, \quad (2.3)$$

Where

$$\mu = \frac{\delta F}{\delta \psi} = [r\psi + \lambda({q_0}^2(r) + \nabla^2)^2\psi - \psi^2 + \psi^3] \quad (2.4)$$

is the chemical potential.

This choice permits the study of pattern relaxation without imposing a particle-conservation constraint. The resulting dynamics evolve the density field toward lower free-energy configurations.

2.2 Stochastic characteristic wavenumber

The principal modification introduced in this work is the replacement of the fixed characteristic wavenumber by a stochastic quantity,

$$q_0(r, t) = \frac{q_c}{1+\delta\eta(r,t)}. \quad (2.5)$$

Here, q is the reference characteristic wavenumber, δ controls the magnitude of the perturbation, and $\eta(r, t)$ is a stochastic field satisfying

$$\langle \eta(r, t) \rangle = 0 \quad (2.6)$$

and

$$\langle \eta(r, t)\eta(r', t') \rangle = \delta(r - r')\delta(t - t'). \quad (2.7)$$

The parameters are chosen as

$$\lambda = 1,\ q_c = 1, \quad (2.8)$$

with perturbation amplitudes in the range

License: This is an open access article under the CC BY 4.0 license: https://creativecommons.org/licenses/by/4.0/

$$0 \le \delta \le 0.20. \quad (2.9)$$

For $\delta = 0$, the model reduces to the fixed-wavenumber case. Increasing δ introduces increasing fluctuations into the locally preferred structural wavelength. The physical motivation is straightforward. A fixed q favors a globally coherent periodic length scale. Allowing q to fluctuate introduces spatial and temporal variation in this preferred length scale. The system can therefore retain a tendency toward local organization without being forced into a single globally periodic configuration. The resulting mechanism differs from simply perturbing the positions of particles after a crystal has formed. The structural disorder develops during the free-energy evolution itself.

2.3 Computational domain and discretization

The equations are solved numerically in a two-dimensional square domain, $0 \le x \le L$, $0 \le y \le L$.

The largest simulations use $L = 1024$, with a 1024×1024 spatial grid. The temporal discretization time steps uses $\Delta t = 0.01$, with a maximum simulation time of $t = 25000$. Periodic boundary conditions are imposed,

$$\psi(x, y) = \psi(x \pm mL, y \pm mL), \quad (2.10)$$

where m is an integer. The initial density field is generated from random fluctuations,

$$\psi(x, y, t = 0) = \xi_{x,y} \quad (2.11)$$

where ξ , is a random field that is uniformly distributed $\xi \in (-0.5, 0.5)$.

The fourth-order differential equation is reduced to a system involving second-order spatial derivatives, with the Laplacian evaluated using a central finite-difference approximation. The temporal evolution is advanced using Euler algorithm.

Simulations were performed using high-performance computing resources at the Centre for High Performance Computing (CHPC) supercomputers.

2.4 Simulation protocol

For each parameter set, independent simulations were initialized from different random density fields. The thesis reports 30 independent simulations for the principal parameter sets and more than 15 simulations for each parameter combination used in constructing the state diagram.

The free-energy evolution was monitored throughout the simulations. At late times the relative change in free-energy density became negligible, with the simulations being terminated at $t = 25000$ for the principal analysis.

At approximately $t = 400$, the simulations already exhibited negligible free-energy changes according to the criterion used in the original study; $t = 25000$ was therefore justifiably used as a late-time state for structural characterization.

3. STRUCTURAL CHARACTERIZATION

3.1 Point-pattern representation

The PFC simulations produce continuous density fields rather than explicit particle coordinates. To characterize the resulting structures using point-pattern methods, the high-density regions of the final density field are identified, and their central positions are extracted. These positions provide an effective point representation of the density maxima. The resulting point patterns are subsequently used to calculate local number fluctuations and pair correlations. This transformation allows structural properties of the continuous PFC field to be connected to the established statistical framework used for hyperuniform point patterns.

3.2 Number variance

Hyperuniformity is characterized by the scaling of density fluctuations at large length scales. In real space, a sampling window of characteristic radius R, the local number variance is

$$\sigma_N^2(R) = \langle N(R)^2 \rangle - \langle N(R) \rangle^2. \quad (3.1)$$

For a conventional disordered system in two dimensions, the asymptotic scaling is generally proportional to the area,

$$\sigma_N^2(R) \sim R^{d-\alpha}, \quad \alpha = 0. \quad (3.2)$$

For a hyperuniform system, the number variance grows more slowly. Class-I hyperuniform systems exhibit

$$\sigma_N^2(R) \sim \begin{cases} R^{d-1}, & \alpha > 1 \text{ (class I)} \\ R^{d-1} lnR, & \alpha = 1 \text{ (class II)} \\ R^{d-\alpha}, & 0 < \alpha < 1 \text{ (class III)} \end{cases} \quad (3.3)$$

in two dimensions. For the simulations reported here, more than 6000 sampling centers were randomly distributed within the system without overlapping the finite system boundary. The largest sampling radius was restricted to

$$R_{\max} = \frac{L}{2}. \quad (3.4)$$

3.3 Pair-correlation function

The pair-correlation function $g\,(r)$provides a real-space measure of structural correlations.

For a statistically homogeneous point pattern,

$$g_2(r) = \frac{1}{4\pi r^2} \frac{1}{N\rho} \sum_{i=1}^{N} \sum_{k \ne i}^{N} \langle (r - |\boldsymbol{r}_k - \boldsymbol{r}_i|) \rangle \quad (3.5)$$

measures the probability of finding a particle at separation r from a reference particle relative to the probability expected for an uncorrelated distribution. A conventional uncorrelated system approaches $g\,(r) \to 1$ at large separation.

License: This is an open access article under the CC BY 4.0 license: https://creativecommons.org/licenses/by/4.0/

In a crystal, by contrast, the pair-correlation function contains persistent peaks associated with the repeated long-range periodic structure. Consequently, the combination of pronounced short-range peaks and $g(r) \rightarrow 1$ at large r provides evidence for local structural order without conventional long-range translational ordering.

4. RESULTS

4.1 Formation of disordered patterned states

Starting from random initial density fields, the system initially resembles a homogeneous liquid-like state. As the free energy decreases, spatial modulation develops and a patterned state emerges.

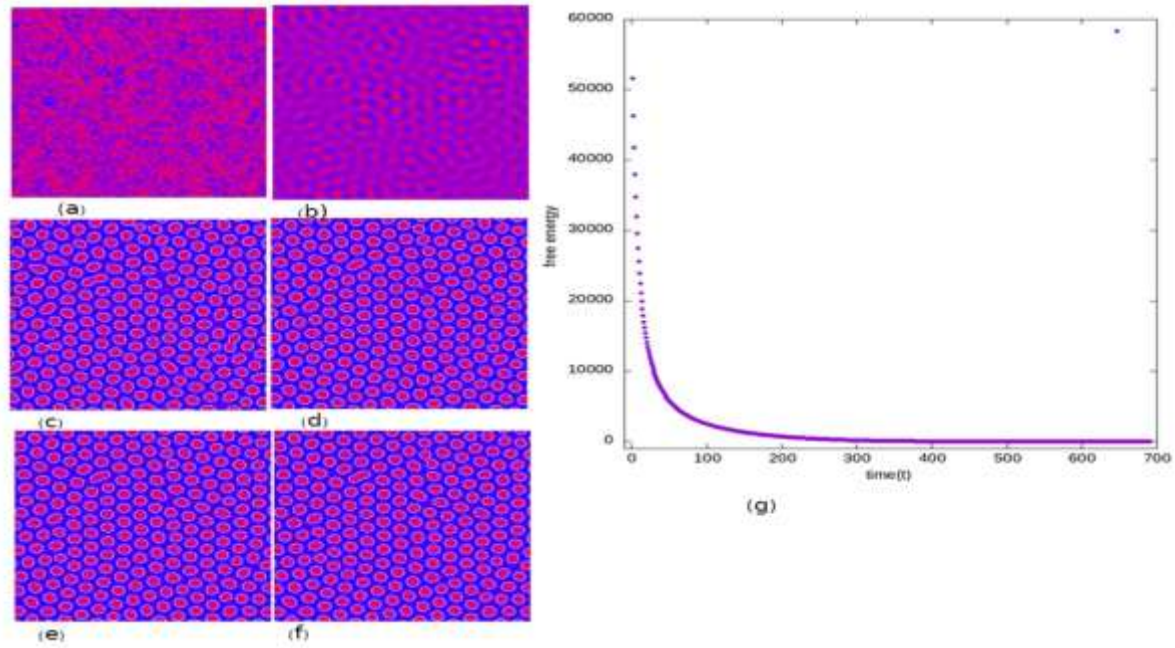


Figure 4.1 Showing 1302 section of the 10242 snapshots of the patterns at (a) t = 0, (b) t = 4000, (c) t = 8000, (d) =15000, (e) t = 20000, (f) t = 250000, and (g) is the free energy density versus computation time for the parameters r = −1 and δ = 0.10 .

For example, simulations at $r = -1$ and $\delta = 0.10$ show the progressive formation of a patterned structure as the simulation evolves. The density field develops spatial organization while the free energy decreases toward a late-time state.

The simulations show that different random initial conditions evolve toward the same broad structural state for a fixed set of model parameters. This behavior indicates that the observed morphology is not simply a consequence of a particular initial random realization. The late-time structures retain recognizable local triangular organization but lack the obvious global periodicity of an ideal triangular crystal. This is the first indication that stochastic modulation of the characteristic wavenumber can transform the conventional PFC crystalline tendency into a disordered patterned state.

4.2 Effect of stochastic perturbation amplitude

The perturbation amplitude δ controls the magnitude of the stochastic fluctuations in the preferred characteristic wavenumber. At $\delta = 0$, the model has a fixed characteristic wavenumber and produces the conventional ordered pattern associated with the selected PFC parameter regime. Increasing δ introduces increasing local variation in the preferred structural wavelength.

The resulting structures remain locally organized, but the global periodicity becomes progressively disrupted. For perturbations up to $\delta = 0.20$, the system retains a disordered triangular-like morphology suitable for further hyperuniformity analysis.

License: This is an open access article under the CC BY 4.0 license: https://creativecommons.org/licenses/by/4.0/

Corresponding Author: Nkosikhona Dlamini

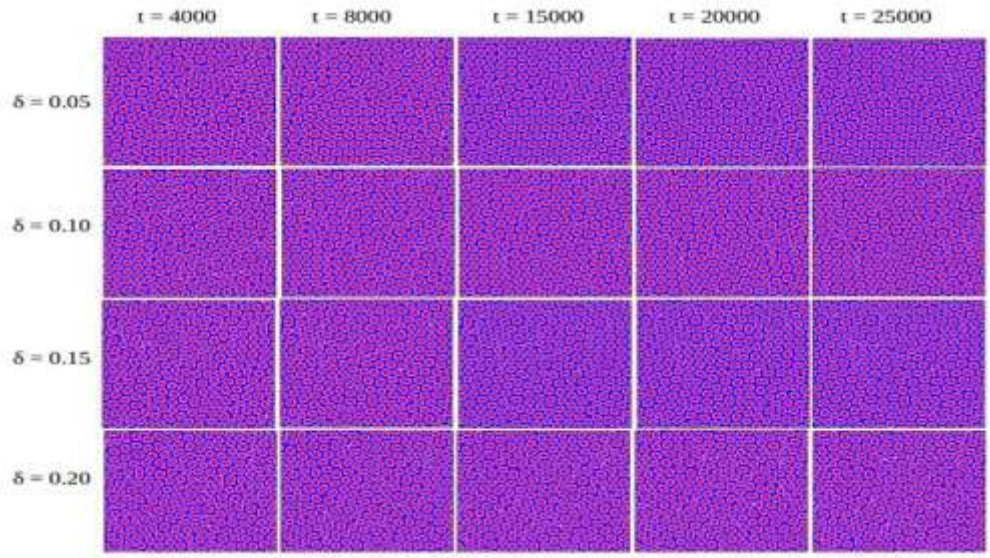


Figure 4.2: Shows evolution snapshots of the systems at t = 4000, t = 8000, t = 15000, t = 20000 = and t = 25000 for fixed r = −0.1, as observed for different noise strength δ values.

The results therefore indicate that stochastic modulation does not immediately destroy local organization. Instead, it produces a regime in which local order and large-scale disorder coexist.

4.3 Hyperuniformity from number-variance scaling

The final configurations were converted into point patterns and analyzed using the local number variance.

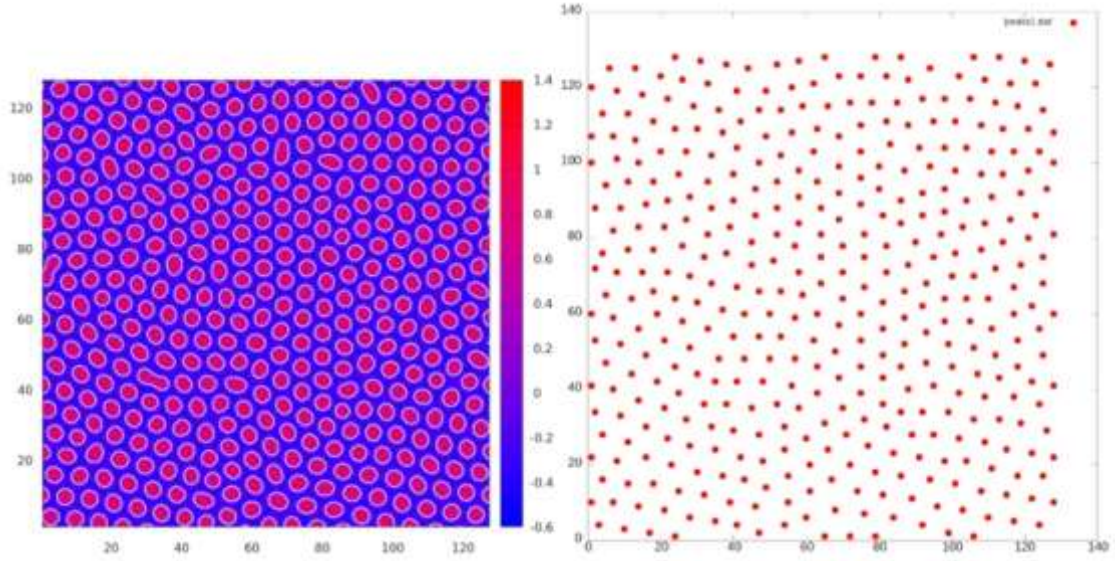


Figure 4.3: Left window shows density scalar fields realization of the Swift-Hohenberg equation for r = −0.1 and δ = 0.15 at t = 25000. Right window shows point pattern generated by reducing the high-density locations in left window.

For δ = 0, 0.10, 0.15, 0.20, the measured number variance exhibits an approximate with power-law scaling,

$$\sigma_N^2(R) \sim R^{1.5} \ , \ m \simeq 1.5. \qquad (4.1)$$

In a two-dimensional system this corresponds to α = 0.5. This is the characteristic scaling consistent with class-III hyperuniformity (0 < α < 1), indicating a weakest hyperuniformity where the variance grows slower than the volume but faster than the surface area.

License: This is an open access article under the CC BY 4.0 license: https://creativecommons.org/licenses/by/4.0/

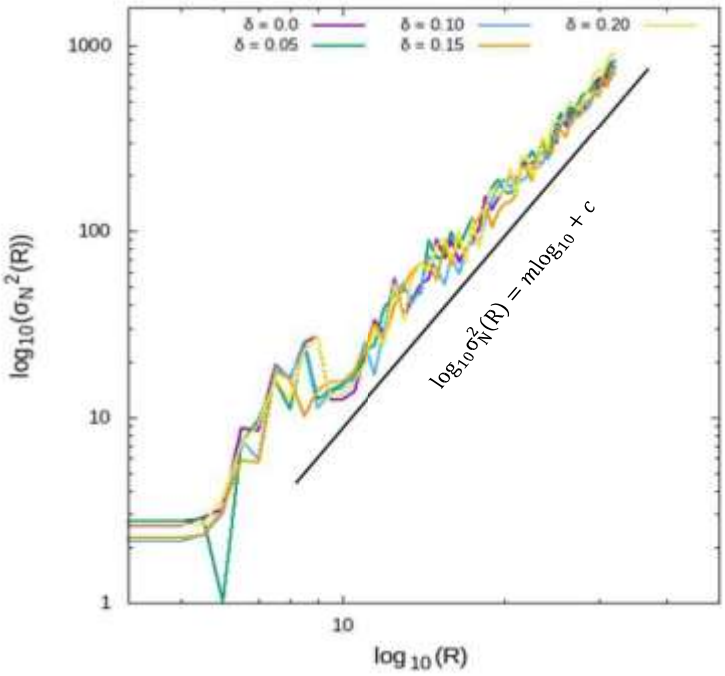


Figure4.4: Logarithm of the number variance $\sigma = N(R)$ versus the logarithm of the window radius R for δ = 0.0, δ = 0.10, δ = 0.15, and δ = 0.20 at t = 25000, r = −0.1. The solid line is guide that illustrates the linear dependence of the number variance with the radius of sampling window.

The result is significant because the corresponding density fields are not conventional periodic crystals. The stochastic-wavenumber mechanism therefore produces structures that retain strong suppression of long-wavelength density fluctuations despite the loss of obvious translational periodicity.

The numerical results support the interpretation that the generated triangular-like disordered structures are hyperuniform over the range of perturbation amplitudes investigated.

4.4 Persistence of short-range order

The pair-correlation functions provide complementary information about the structural organization. For the different stochastic perturbation amplitudes, the first several peaks of $g\ (r)$ remain approximately at the same positions. In particular, the first prominent peak occurs around

$$R/a \approx 6.3. \qquad (4.2)$$

The persistence of the first four peaks indicates that the local structural environment remains relatively stable as the stochastic perturbation amplitude is increased.

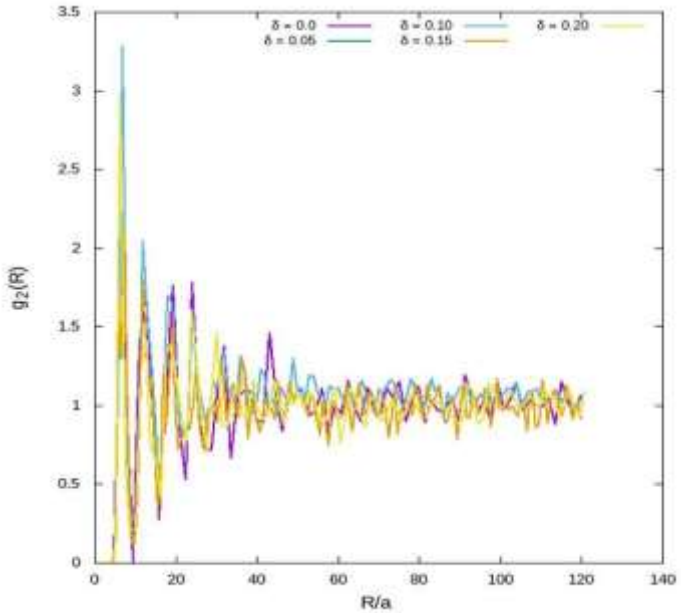


Figure 4.5: Pair correlation functions $g\ (R)$ of the systems under varying noise amplitudes δ.

License: This is an open access article under the CC BY 4.0 license: https://creativecommons.org/licenses/by/4.0/

At larger distances, $g(R) \rightarrow 1$. This behavior indicates that the local correlations decay and that conventional long-range translational order is absent. The combined number-variance and pair-correlation results therefore reveal two apparently contrasting features robust short-range structural order and suppressed long-range density fluctuations without convectional periodic order. This combination is characteristic of the hidden structural organization associated with disordered hyperuniformity.

4.5 Free-energy relaxation

The formation of the patterned structures is accompanied by a decrease in the system free energy. For the different perturbation amplitudes investigated at $r = -0.1$, the free-energy evolution follows an approximate power-law form

$$E(t) \sim t^{x}. \tag{4.3}$$

The simulations yield

$$x \approx -1.26 \pm 0.08$$

The free-energy evolution exhibits an obvious dependence on the perturbation amplitude δ. For larger perturbations, the system undergoes a relatively smooth relaxation towards a long-time state, with the intermediate-time decay approximately following an algebraic form, $E(t) \sim t^{\cdots}$. In contrast, the cases with smaller perturbations exhibit a more complex relaxation pathway. These trajectories initially decreased to a metastable low energy state before undergoing a subsequent transition to a second, lowerenergy state at later times. This two-stage relaxation suggest the presence of competing metastable configurations or energy minima, with the system requiring additional time to reorganize from the initially accessed state into a lower-energy configurations. The observed behavior indicates that the perturbation amplitude influences not only the rate of energy relaxation but also the pathway through which the system approaches its final state.

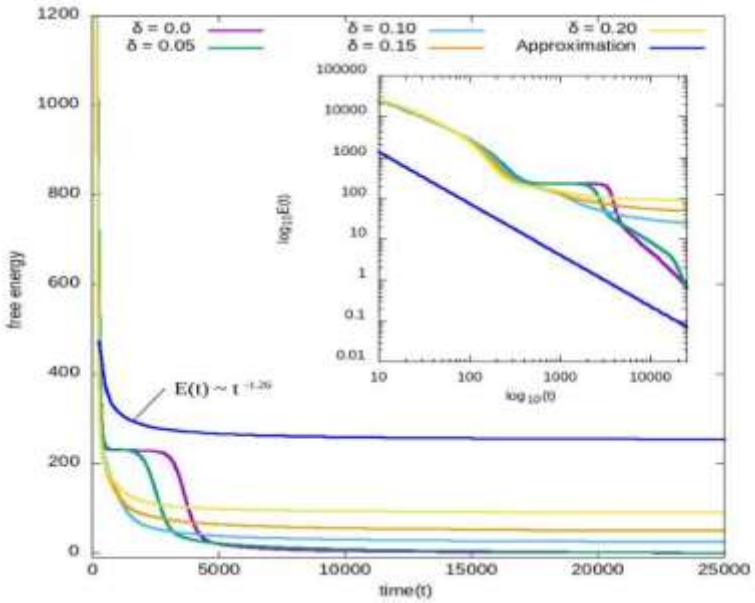


Figure 4.6: Shows the insert of the long-time free-energy evolution on a log-log Scale. The blue line represents a power-law reference, $E(t) \sim t^{\pm \cdot}$, which captures the overall decay trend of the free energy over the approximately algebraic regime. Deviations from this scaling at early and late times reflect the crossover towards the corresponding long-time states

The characteristic length scale associated with the evolution is reported to grow approximately as

$$L_E \sim t^{0.63}, \tag{4.4}$$

which is close to

$$L_E \sim t^{3/5}. \tag{4.5}$$

Thus, the free-energy relaxation can be summarized approximately as

$$E(t) \sim t^{-6/5},\ L_E(t) \sim t^{3/5}. \tag{4.6}$$

These results indicate that the stochastic perturbation changes the spatial organization of the resulting state without substantially changing the late-stage scaling behavior of the free-energy relaxation. The scaling of the characteristic function indicates that the unconserved system is growing faster than the classical diffusive scaling.

4.6 State diagram in the $r - \delta$ parameter space

To examine the robustness of the resulting structures beyond a single parameter choice, simulations were performed over $r \in (-0.8, 0.1)$ and $\delta \in (0, 0.2)$.

More than 15 simulations were performed for each parameter set using random initial conditions. Four broad states were identified: homogeneous liquid-like states, triangular patterned states coexistence states and stripe states. The triangular state occurs over a finite region of the parameter

License: This is an open access article under the CC BY 4.0 license: https://creativecommons.org/licenses/by/4.0/

space. For smaller perturbation amplitudes, changing δ at fixed r does not substantially change the resulting state. At larger perturbation amplitudes, particularly for $\delta \gtrsim 0.15$, the system increasingly enters coexistence regions.

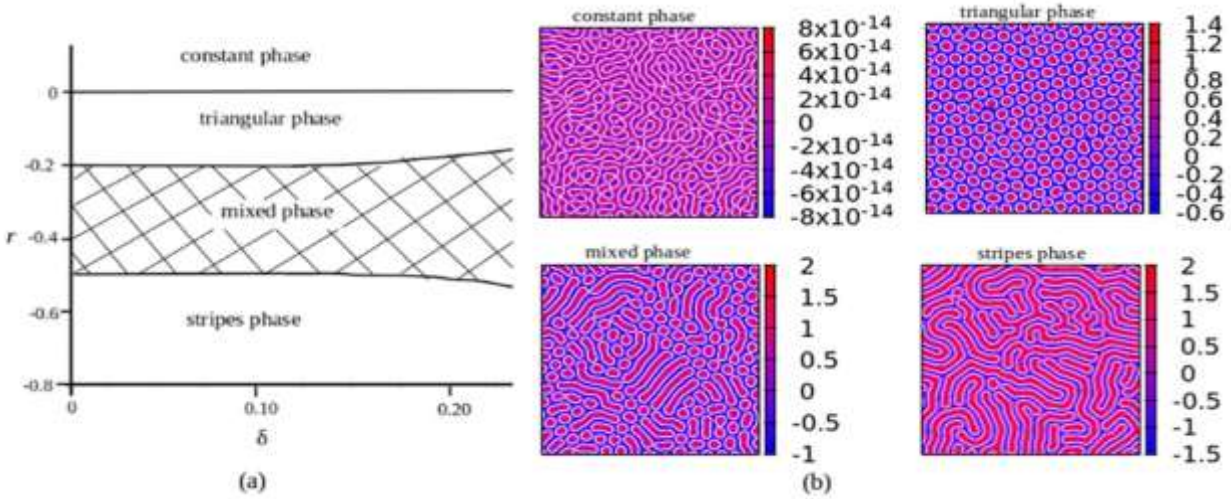


Figure 4.7: (a) Phase diagram of resulting phases that were obtained from initial conditions in 2D minimization along the $r - \delta$ plane. The hatched regions show the coexistence phase, (b) realizations corresponding to the different phases of the phase diagram

The numerical state diagram therefore demonstrates that the stochastic-wavenumber modification does not immediately destroy the underlying pattern-forming behavior. Instead, the perturbation produces a range of disordered triangular-like states before sufficiently large perturbations drive the system toward qualitatively different morphologies.

5. DISCUSSION

The principal result of this study is that stochastic modulation of the characteristic wavenumber provides a simple mechanism for producing disordered hyperuniform structures within a PFC framework.

The mechanism differs conceptually from imposing disorder on a pre-existing crystal. In the present model, the preferred structural wavelength itself fluctuates during the evolution. Consequently, the system continuously experiences a competition between the tendency of the PFC free energy to establish a characteristic pattern and the stochastic spatial and temporal modulation of the characteristic wavelength.

This competition produces a useful structural regime. At short distances, the system retains a well-defined local organization, as demonstrated by the persistence of the first several peaks in $g\,(r)$. At large distances, the pair correlation function approaches unity, indicating the disappearance of conventional long-range translational correlations.

At the same time, the number-variance analysis shows

$$\sigma_N^2(R) \sim R^{1.5}, \qquad (5.1)$$

indicating that large-scale density fluctuations remain suppressed corresponding to class III hyperuniformity. The combination of these observations provides evidence that the resulting structures are not simply ordinary disordered patterns. Instead, they retain hidden large-scale organization characteristic of hyperuniform systems. The robustness of this behavior to perturbations is also notable. The number-variance scaling remains approximately linear for the investigated perturbation amplitudes up to $\delta = 0.20$, while the short-range pair-correlation structure remains relatively stable. This suggests that the hyperuniform state is not associated with a single finely tuned value of the stochastic perturbation. Rather, it occupies a finite range of the model parameter space. The dynamic results provide a second important aspect of the study.

The free-energy evolution follows an approximate power law with exponent approximately $-\frac{6}{5}$, while the associated length scale grows as $L_E \sim t^{0.63}$. The approximate correspondence between these exponents suggests a consistent late-stage scaling regime in which progressively larger domains of the disordered hyperuniform pattern develop during relaxation.

The resulting approach is computationally attractive because PFC models operate at microscopic length scales while allowing access to diffusive time scales. This makes the framework potentially useful for investigating pattern formation processes that would be computationally expensive using fully atomistic molecular-dynamics simulations.

7. CONCLUSIONS

We have investigated a modified two-dimensional phase-field-crystal model in which the characteristic wavenumber is subjected to stochastic perturbations. The stochastic-wavenumber PFC generates disordered triangular-like structures. Starting from random initial conditions, the model evolves toward patterned states that retain local organization while lacking obvious conventional longrange periodicity. The resulting structures exhibit hyperuniform number-variance scaling. For perturbation amplitudes up to $\delta = 0.20$, the measured number variance approximately follows $\sigma\,(R) \sim R^{\cdot}$, consistent with class-III hyperuniform behavior in two dimensions. The first several peaks in the pair-correlation function remain approximately unchanged as the stochastic perturbation amplitude is varied. This gives evidence that short-range structural order is robust.

License: This is an open access article under the CC BY 4.0 license: https://creativecommons.org/licenses/by/4.0/

Conventional long-range spatial correlations are suppressed. The pair-correlation function approaches unity at large separation, distinguishing the resulting structures from conventional crystalline order. The free-energy relaxation follows an approximate power law. The simulations give $E(t) \sim t^{\cdot}$, with the associated length scale approximately obeying $L(t) \sim t^{\cdot}$. The disordered hyperuniform state is robust over a finite perturbation range. The numerical state diagram shows persistence of the triangular state for a range of perturbation amplitudes, while sufficiently large perturbations promote coexistence and other patterns.

Overall, the results demonstrate that introducing stochasticity into the characteristic wavenumber provides a simple route for generating and studying disordered hyperuniform states using phase-field-crystal dynamics. The approach combines structural disorder with suppressed long-wavelength density fluctuations and provides access to diffusive pattern-formation dynamics. Future work should extend the model to three dimensions, curved geometries, and other PFC pattern-forming regimes, including stripe states. Further characterization should also include reciprocal-space structure factors, quantitative uncertainty estimates for scaling exponents, and systematic finite-size analysis.

DATA AND CODE AVAILABILITY

The original study includes a Fortran implementation of the stochastic-wavenumber Swift–Hohenberg/PFC calculation in the thesis appendix. For journal submission, the computational code and, where possible, representative simulation data should be deposited in an appropriate public repository.

ACKNOWLEDGMENTS

The authors acknowledge the Centre for High Performance Computing (CHPC) Lengau, for computational resources used in the numerical simulations. N.D. acknowledges the guidance and supervision provided by S. K. Mkhonta during the development of the original MSc research.

AUTHOR CONTRIBUTIONS

N.D. developed and performed the numerical investigation and analyzed the simulation results. S.K.M. supervised the research and contributed to the formulation and interpretation of the study. S.T. contributed to the development and discussion of the structural order analysis. All authors contributed to the interpretation of the results and revision of the manuscript.

CONFLICT OF INTERESTS

The authors declare no competing interests.

FUNDING

This research received no specific grant from any funding agency in the public, commercial, or not-for-profit sectors.

DATA ACCESS STATEMENT

The data and computational code supporting the findings of this study are openly available in Figshare at 10.6084/m9.figshare.34063671. The repository contains the phase-field-crystal simulation code, simulation data, used to generate the results presented in this manuscript.

REFERENCES

1) S. Torquato, “Inverse optimization techniques for targeted self-assembly,” Soft Matter 5, 1157 (2009).
2) R. D. Batten, F. H. Stillinger, and S. Torquato, “Classical disordered ground states: Super-ideal gases and stealth and equi-luminous materials,” J. Appl. Phys. 104, 033504 (2008).
3) S. Torquato and F. H. Stillinger, “Local density fluctuations, hyperuniform systems, and order metrics,” Phys. Rev. E 68, 041113 (2003).
4) C. E. Zachary and S. Torquato, “Hyperuniformity in point patterns and two-phase heterogeneous media,” J. Stat. Mech. P12015 (2009).
5) S. Torquato, “Hyperuniformity and its generalizations,” Phys. Rev. E 94, 022122 (2016).
6) S. Torquato, “Hyperuniform states of matter,” Phys. Rep. 745, 1–95 (2018).
7) A. Gabrielli, “Point processes and stochastic displacement fields,” Phys. Rev. E 70, 066131 (2004).
8) A. Gabrielli, M. Joyce, and S. Torquato, “Tilings of space and super-homogeneous point processes,” Phys. Rev. E 77, 031125 (2008).
9) E. Lomba, J.-J. Weis, and S. Torquato, “Disordered hyperuniformity in two-component non-additive hard disk plasmas,” Phys. Rev. E 96, 062126 (2017).
10) E. Lomba, J.-J. Weis, and S. Torquato, “Disordered multi-hyperuniformity derived from binary plasmas,” Phys. Rev. E 97, 010102(R) (2018).
11) Y. Jiao, T. Lau, H. Hatzikirou, M. Meyer-Hermann, J. C. Corbo, and S. Torquato, “Avian photoreceptor patterns represent a disordered hyperuniform solution to a multiscale packing problem,” Phys. Rev. E 89, 022721 (2014).
12) G. Zhang, F. H. Stillinger, and S. Torquato, “The perfect glass paradigm: Disordered hyperuniform glasses down to absolute zero,” Sci. Rep. 6, 36963 (2016).
13) G. Zhang, F. H. Stillinger, and S. Torquato, “Classical many-particle systems with unique disordered ground states,” Phys. Rev. E 96, 042146 (2017).
14) S. Torquato, G. Zhang, and F. H. Stillinger, “Ensemble theory for stealthy hyperuniform disordered ground states,” Phys. Rev. X 5, 021020 (2015).
15) S. Yu, C.-W. Qiu, Y. Chong, S. Torquato, and N. Park, “Engineered disorder in photonics,” Nat. Rev. Mater. 6, 226–243 (2020).
16) K. Vynck, M. Burresi, F. Riboli, and S. D. Wiersma, “Photonic management in two-dimensional disordered media,” Nat. Mater. 11, 1017–1022 (2012).

License: This is an open access article under the CC BY 4.0 license: https://creativecommons.org/licenses/by/4.0/

17) W. Man, M. Florescu, K. Matsuyama, P. Yadak, S. Torquato, P. J. Steinhardt, and P. Chaikin, “Experimental observation of photonic bandgaps in hyperuniform disordered materials,” Conference on Lasers and Electro-Optics (2010).
18) K. R. Elder and M. Grant, “Modeling elastic and plastic deformations in nonequilibrium processing using phase field crystal,” Phys. Rev. E 70, 051605 (2004).
19) K. R. Elder, N. Provatas, J. Berry, P. Stefanovic, and M. Grant, Phys. Rev. B 75, 064107 (2007).
20) H. Emmerich, H. Löwen, R. Wittkowski, T. Gruhn, G. I. Tóth, G. Tegze, and L. Gránásy, “Phase-field-crystal models for condensed matter dynamics on atomic length and diffusive time scales: an overview,” Adv. Phys. 61, 665–743 (2012).
21) L. Q. Chen, “Phase-field models for microstructure evolution,” Annu. Rev. Mater. Res. 32, 113–140 (2002).
22) J. W. Cahn and J. E. Hilliard, “Free energy of a nonuniform system. I. Interfacial free energy,” J. Chem. Phys. 28, 258– 267 (1958).
23) J. Swift and P. C. Hohenberg, “Hydrodynamic fluctuations at the convection instability,” Phys. Rev. A 15, 319–328 (1977).
24) A. Emdadi, M. A. Zaeem, and E. Asadi, “Revisiting phase diagrams of two-mode phase field crystal models,” Comput. Mater. Sci. 123, 139–147 (2016).
25) D. Taha, S. R. Dlamini, S. K. Mkhonta, K. R. Elder, and Z.-F. Huang, “Phase ordering, transformation, and grain growth of two-dimensional binary colloidal crystals: A phase field crystal modelling,” Phys. Rev. Mater. 3, 095603 (2019).
26) L. Gránásy, G. Tegze, G. I. Tóth, and T. Pusztai, “Phase-field crystal modelling of crystal nucleation, heteroepitaxy and patterning,” Philos. Mag. 91, 123 (2011).
27) R. Dreyfus, Y. Xu, T. Still, L. A. Hough, A. Yodh, and S. Torquato, “Diagnosing hyperuniformity in two-dimensional, disordered, jammed packings of soft spheres,” Phys. Rev. E 91, 012302 (2015).
28) S. Atkinson, G. Zhang, A. B. Hopkins, and S. Torquato, “Critical slowing down and hyperuniformity on approach to jamming,” Phys. Rev. E 94, 012902 (2016).
29) D. Hexner and D. Levine, “Hyperuniformity of critical absorbing states,” Phys. Rev. Lett. 114, 110602 (2015).
30) S. Tsabedze, N. Dlamini, and S. K. Mkhonta, “Regularity and resilience of short-range order in uniformly randomized lattices,” J. Phys. Commun. 6, 105008 (2022).

License: This is an open access article under the CC BY 4.0 license: https://creativecommons.org/licenses/by/4.0/

Corresponding Author: Nkosikhona Dlamini